CHAPTER 1

INTRODUCTION

1.1 Overview on precision agriculture

The world population is growing and lands available for agriculture are likely to decrease despite technological improvement that might extend the boundaries of land that can support agriculture development. High intensity of land usage for agriculture and changes in land used had resulted serious consequences to the environment. A larger world population increases challenges on land management at the same time ensure agriculture sustainability, food security and preserved environment through precision agriculture (PA) (Oliver *et al*., 2013). PA is one of the top ten revolutions in agriculture, and it has been implemented commercially since the 1990's (Mulla, 2013).

PA methodologies and technologies are the most reliable and cost effective approach for simultaneous sustainable environmental management and efficient crop production (Gertsis *et al.*, 2013). It optimizes agricultural production, improve productivity, crop quality and food traceability and at the same time reduce undesirable impact on the environment and improve sustainability (Oliver *et al*., 2013). PA yields profitable farming as it implements precise tracking and improve production with opportunities of proper management customized by various factors *e.g*. soil variability, crop variability, variability in fertilizers and pesticides application and field topography variability.

In conventional agriculture, fertilizers, herbicides and insecticides are applied uniformly across the field at a given time without any information on the amount required based on both spatial and temporal factors. This resulted over-application at certain area and under-application in others. As example, over-application of fertilizers especially nitrate (NO_3^-) and phosphate (PO_4^{3-}) causes the nutrients to move out of the field to ground water, surface water and other land areas where they are not needed (Oliver *et al*., 2013). In fertilizers application, the principles fertilizers are nitrate, phosphate and potassium, while nitrate and phosphate have the greatest effect on the environment (Oliver *et al*., 2013). Nitrate and phosphate from fertilizers accumulate in surface water (lake, river and ocean) leading to eutrophication. PA management ensures application of fertilizers and pesticides at the specific area and time when they are needed by crops with precise amount required.

1.2 Importance of the study

Soil sensors have been used to perform soil fertility check and fertilizers content in soil *i.e*. nitrate, phosphate and potassium as part of PA technologies. When the test results are obtained, it is used as a reliable basis for the plant fertility management where application of fertilizers program can be planned and implemented efficiently. In parallel with the expansion of PA, various attempts to develop soil sensors (Cranny, 2012; Kweon, 2013 and Maleki, 2007) had been reported and reviewed to increase the effectiveness of PA (Adamchuk *et al*., 2004). Robust, low-cost and preferably on-the-go and real-time sensing systems are needed for implementing in various PA technologies. Numerous sensors based on electrical and electromagnetic (Blonquist Jr. *et al*., 2006; Murata *et al.*, 2014), optical (Kweon *et al*., 2013) and radiometric (Escorihuela *et al*., 2010), mechanical (Bogrekci *et al*., 2007), acoustic, pneumatic and electrochemical measurement concepts have been produced (Adamchuk *et al*., 2004). Electrochemical

sensors have also been developed with ion-selective membrane that produces a voltage output in response to the activity of selected ions (nitrate, phosphate, potassium *etc.*) for the purpose of nutrients content analysis in soil for the crops benefit.

1.3 Objectives of the study

The purpose of this study is to develop nitrate electrochemical sensor based on ion-selective electrode (ISE) for measurement of NO_3^- ion using printed circuit board (PCB) modify with carbon paste. The sensor is used in soils measurement to obtain the nutrient content of NO_3^- at the specific area and time. The automated fertilizer spray system will compute how much fertilizers require to the affected area and supply it with precise amount to promote crop's growth and health, while avoiding over-fertilization that would impact the environmental.

1.4 Scope of study

The sensor development begins with the preparation of electrode and characterization of conducting carbon electrode followed by electropolymerization of conducting polymer where pyrrole monomer was polymerized to polypyrrole (PPy) using potentiostat (Brand: AutoLAB) via chronopotentiometry method. The next step was characterization of PPy film on the carbon layer using cyclic voltammetry method by scanning the modified electrode from -1.0 to +0.4 V *vs*. Ag/AgCl reference electrode. The ion-selective membrane comprises of polymer materials was prepared and the sensor testing was carried out to evaluate its performance as nitrate ISE sensor.

CHAPTER 2

LITERATURE REVIEW

This chapter describes the relationship between nitrogen and its derivatives related to plants requirement. The chapter also shares the importance of precision agriculture as in having periodical monitoring the level of nitrate in soil for field application to avoid excessive nitrate fertilizer which will give environmental impact. Thus this is where nitrate sensor comes in for the purpose of measuring the nitrate content in soil. The chapter explains the principle of the nitrate sensor, its development, materials of construction and the importance and function of each material. This sensor will be tested for the functionality and performance will be described in Chapter 4 later.

2.1 Role of nitrogen and its derivatives in soil

Nitrogen is one of the most essential nutrients for plants growth. Nitrogen source for plant is obtained mainly from soil solution where it presents in different forms. Majority of nitrogen in soils (>98%) is in organic matter and only a small fraction is in inorganics form (nitrate) that is produced via biological processes involving soil microorganisms (Dechorgnat *et al.,* 2011). Excessive fertilizer as nitrate supply in agriculture causing it to leach out and also release to the environment which contribute to surface water eutrophication, increased emissions of the greenhouse gas nitrous oxide (N_2O) from agricultural soils, and soil acidification (Zhou, *et al.*, 2012). The leaching out of nitrate has also resulting spatial and temporal variable of nitrate concentration in soil solutions (Dechorgnat *et al.,* 2011). The variation of nitrate concentration is a major factor to be considered for efficient fertilizer addition to obtain precise amount required which is

offered in PA technologies. In parallel, PA applications have been deployed in the fields as closed loop system equipped with computer for signal processing and data analysis, auto calibration system and network system.

2.2 Electrochemical sensor

Electrochemical sensor is a very important sensor whose response is the results of interaction between electricity and chemistry by detecting the presence of a chemical quantitatively and converting the chemical information into an easily recognizable signal (electrical) (Vetelino *et al.*, 2011). Chemical sensors contain two basic functional units *i.e.* the receptor part and the transducer part. Receptor transforms into a form of energy which may be measured by the transducer. Transducer for electrochemical sensor measures the energy signal through potentiometric, voltammetric (amperometric) and coulometric (Dimeski *et al.*, 2010). Among them, potentiometric is the most commonly used technique and it involves measurement of potential (voltage) produced by the cell under equilibrium condition (Dimeski *et al.*, 2010). Potentiometry sensors are simple, robust, inexpensive analytical devices well suited for laboratory and field application (Florinel-Gabriel, 2012). This sensor measures the electrical potential of an electrode when there is no current flowing. The signal is measured as the potential difference (voltage) between the working electrode (nitrate sensor) and the reference electrode (RE).

2.2.1 Reference electrode, RE

Reference electrode, RE is needed to provide a defined reference potential. RE is an electrode which has a stable and well-known electrode potential. There are many types of RE available mainly silver/silver chloride (Ag/AgCl), saturated calomel electrode (SCE) and normal hydrogen electrode (NHE) (Yin *et al.*, 2013). Ag/AgCl electrodes are available in a wide range of designs, shapes and sizes. Ag/AgCl is preferably be used as it is the most convenient and commercially available (Vonau, *et al.*, 2010), it exhibits stable potential, well defined in relation to the potential of the standard hydrogen electrode (SHE) (Vonau *et al.*, 2010), easy for manipulation, green chemistry and safe to use (Yin, *et al.*, 2013). Double-junction Ag/AgCl electrodes are commonly preferred since they minimize contact between the analyte sample and the high concentration of potassium chloride (KCl) electrolyte as the reference electrode solution (Telting-Diaz *et al*., 2006).

2.2.2 Ion-selective electrode, ISE

Working electrode for electrochemical sensor is a construction of ion-selective electrode (ISE). ISE is an electrochemical sensor, based on thin films or ion-selective membranes as recognition element. ISE had been widely used in clinical, environmental analysis and process control (Amemiya, 2007). ISE has unique characteristics such as small in size, easy to operate, portable and low cost (Marco *et al.*, 2013). Multiple designs of ISEs with size ranging from centimeter-long probes to miniaturized sensor with solid-state chemical sensor arrays had been reported with potentiometric concept which has become increasingly important in biomedical, industrial and environmental application fields (Telting-Diaz *et al*., 2006). ISEs utilize potentiometric method as the electrical potential measures ion, either in solution or in the gas phase, provides accurate ion

activity value. A potentiometric ISE has simple design, adequate selectivity, low detection limit, high accuracy, fast response, non-toxicity (Huang *et al*., 2012) and wide concentration range of applications (Frag *et al.*, 2012). In potentiometric method, potential of an ISE as working electrode (WE) varies depending on the concentration of the analyte, while the potential arising reference electrode is ideally a constant (refer Figure 2.1).

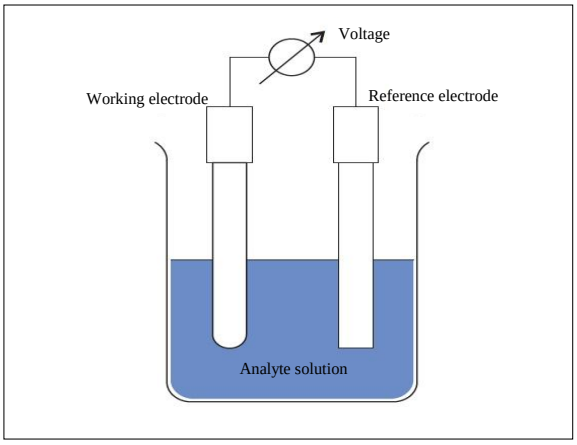

Figure 2.1: Measurement setup for ion-selective electrode potentiometric cell.

ISEs work on the basic principal of the galvanic cell. By measuring the electric potential generated across a membrane by nitrate ions, and comparing it to a reference electrode (RE), a net charge is determined and value is observed from the meter used. The potential of a galvanic cell containing a membrane observed as shown in equation [1] below;

$$E_{cell} = E_{ISE} - E_{reference} \qquad [1]$$

The potential for the cell is equivalent to the potential of the ISE minus the potential of the RE. E_{ISE} is composed of two potentials generating system *i.e.* the potential of internal Ag/AgCl reference electrode, $E_{Ag/AgCl}$ and the membrane potential E_m. The Ag/AgCl RE produces half-cell reaction as below;

$$AgCl \Leftrightarrow Ag^{+} + Cl^{-} \quad [2]$$

The measurement of E_{cell} *i.e.* total potential of the system is based on phenomenon expressed as below Nernst equation;

$$E_{cell} = E^{0}_{Ag/AgCl} + (2.303RT/zF)(\log a) \quad [3]$$

where $E^{0}_{Ag/AgCl}$ is the potential of the Ag/AgCl reference electrode and internal solution (297.15mV), R is referred to gas constant (8.316 $J^{-1}mol^{-1}deg^{-1}$), T is temperature of the system in Kelvin, z is the charge of the chloride ions (-1), F is the Faraday constant (96,485 C. mol^{-1}) and a activity of ions in analyte solution (Buck *et.al.*, 1994) which is the concentration.

Based on Nernst equation, ideal slope for the ISE sensors are listed below;

$[M^{+}]$ or $[M^{-}]$ = 59.16 mV/decade or -59.16 mV/decade [4]

$[M^{2+}]$ or $[M^{2-}]$ = 29.6 mV/decade or -29.6 mV/decade [5]

$[M^{3+}]$ or $[M^{3-}]$ = 19.7 mV/decade or -19.7 mV/decade [6]

$[M^{4+}]$ or $[M^{4-}]$ = 14.8 mV/decade or -14.8 mV/decade [7]

where M is the type of anion or cation and nitrate sensor ideal slope is defined by equation [4].

2.3 Liquid polymeric membrane

The membrane used in ISE probe can be made of glass, crystalline, liquid (Amemiya, 2007) or polymer materials (Meyerhoff *et al.*, 1986). It allows selective measurement of a wide variety of cations and anions (Meyerhoff *et al.*, 1986). ISE with polymeric membrane is also called liquid membrane and it has wide range of analytes applications (Amemiya, 2007). ISEs offer sensor miniaturization (Quan *et al.*, 2001),

robustness (Telting-Diaz *et al.*, 2006), and good mechanical properties (Telting-Diaz *et al.*, 2006) by using solid ion sensor with polymeric liquid membrane onto electrode surface and eliminates the need of internal solution (Quan *et al.*, 2001). Polymeric membrane is hydrophobic and immiscible with water. The most commonly selected (Osakai, *et al.*, 2012) and used membrane made of plasticized polyvinylchloride (PVC) (Amemiya, 2007).

Tremendous number of PVC membranes used for ISEs development for many ions had been reported (Frag *et al.*, 2012; Dimeski *et al.*, 2010; Marco *et al.*, 2013) while the design of these ISEs were based on trial-and-error (Osakai, *et al.*, 2012). Selectivity of the membrane is determined by the nature and composition of the ion-selective membrane materials used for the electrode. The membrane is also defined as permselective as it measures the specific ions by allowing the ion to permeate through the membrane by ion exchange concept (Bakker, 2005). Liquid or polymeric membranes for an ISE must exhibit ion-exchanger properties and the concentration of analyte in the membrane phase need to remain approximately constant as the analyte concentration for a Nernstian response slope to be observed (Bakker, 2005). Selectivity of ISE is achieved by doping the liquid membrane with a numerous types of lipophilic ion exchanger (salt) or carrier, for example, tridodecylmethylammonium chloride (TDMAC) for anion-selective electrodes or potassium tetrakis (4-chlorophenyl) borate for cation-selective electrodes for the same function to selectively and reversibly forms complexes with analyte (Amemiya, 2007 and Bakker, 2005).

Based on previous work by Zook and his co-workers in year 2009, (Zook *et al.*, 2009) the ISEs polymeric membranes are most commonly consist of 33% poly(vinylchloride) (PVC), 66% plasticizer, and small amounts of a lipophilic ion exchanger (lipophilic salt) and ion exchanger or ionophore. Plasticizer either o-nitrophenyl octyl ether (o-NPOE) or dioctyl sebacate (DOS) decreases the membrane resistance and ensure smooth migration of ions across ion-selective membranes. In general, o-NPOE plasticized membranes have smaller resistances than DOS plasticized due to the concentration of ionic impurities in o-NPOE is much larger than in DOS. Ion-exchanger-based ISE provides a very high selectivity against the counter ions of an analyte but it has lack selectivity against the co-ions. The selectivity against interfering co-ions is primarily determined by hydrophobicity of the ions, whereas the selectivity of anion-exchanger-based ISEs among inorganic anions is defined by Hofmeister series (Amemiya, 2007).

$$ClO_4^- > SCN^- > I^- > NO_3^- > Br^- > Cl^- > HCO_3^- > SO_4^{2-} > F^-$$

2.4 Carbon electrode surface

Solid contact ISEs have a good prospect in generation of potentiometric ion sensors, due to their durability, ease of miniaturization and low maintenance. A solid contact between an electronic conductor and an ion-selective membrane is the essential element for fabricating a stable solid-state polymeric membrane ISE, since its intrinsic property significantly influences the potential stability and reproducibility for long-term use (Yin *et al.*, 2013). The first and a very simple solid contact polymeric sensor was proposed in the early 1970s by Cattrall and Freiser (Cattrall *et al.*, 1971). It comprised of a metal wire coated with an ion-selective polymeric membrane (Makarychev-Mikhailov *et al.*, 2008). In extend, metals such as platinum, gold, palladium and carbon are inert electrode conductors suitably used in ISE as they are functioned to transfer electrons to

or from species in the solution (Telting-Diaz *et al.,* 2006). Various forms of carbons have been use widely as electronic conductor to provide solid contacts with membrane in developing solid state ISE such as carbon-based nanomaterials, nanoparticles and nanoclusters for detection of cations and anions (Yin *et al,* 2013).

Carbon-based materials such as fullerene, three-dimensionally ordered macroporous carbon and carbon nanotubes provide effective and outstanding transducers (Ping *et al*., 2011). These materials are insensitive to oxygen and light, which make them preferable to use with conducting polymers in ISEs (Paczosa-Bator, 2012). In the ISE development, carbon black is a great material that has attracted global interest for both of its fundamental properties and its applications for solid-state ISE. Carbon black, as a form of amorphous carbon has advantages in low production cost, an extremely fluffy fine powder with a large surface area (Paczosa-Bator, 2012), high conductivity and good hydrophobicity (Yin *et al*., 2013). ISE was constructed by using carbon black paste and screen printed on the ISE base material or platform for fabrication of nitrate ISE.

2.5 Conducting polymer

Conducting polymers are reported to be frequently used as ion-to-electron transducers in solid-state ISEs (Bobacka *et al.,* 2007). Conducting polymers provide material foundation for the development of miniaturized and durable solid contact ISE and eliminate the needs of any inner solution (Huang *et al*., 2012). The introduction of conducting polymers (*e.g.* polypyrrole (PPy) and poly(aniline) (PANI)) as internal ion-to-electron transducers have significantly improved the potential stability by unblocking the charge transfer at sensors interfaces (Ping *et al*., 2011). A conducting polymer film

containing specific ion receptors improves durability of the solid-state ISEs (Bobacka *et al.*, 2007). Conducting polymers, such as PANI, PPy, poly(3-n-octylthiophene) (POT) and poly(3,4-ethylenedioxythiophene) (PEDOT) are the polymers of interest to be used as ion-to-electron transducers in ISE (Huang *et al*., 2012). Conducting polymers are deposited by electropolymerisation or solution casting directly on the electronic conductor (Bobacka *et al.*, 2007) or can be part of membrane (PVC or Siloprene)'s composition for mix conductivity (Telting-Diaz *et al*., 2006). Most conducting polymer films are fabricated by electropolymerisation of the monomers on solid electronic conductors (*e.g.* carbon material, platinum, gold) (Bobacka *et al.*, 2007). The application of hydrophobic carbon black as a solid contact with conducting polymer, has significantly prevent formation of interfacial aqueous film between the polymeric membrane and the underlying solid-contact that limits the application of conducting polymers (Paczosa-Bator, 2012).

PPy is one of the most extensively used conducting polymers in sensor design *e.g.* bioanalytical sensors and chemical sensors (Ramanavicius *et al.*, 2006). PPy inhibits high conductivity, chemical and physical stability and has low toxicity of the monomer. Among the various conducting polymers, PPy is one of the most studied due to characteristics of simple preparation, easy deposition from aqueous and non-aqueous media, good adhesion to many types of substrates, high conductivity, high stability in air and aqueous media and being able to control experimental conditions via electrochemical techniques (Patois *et al*., 2012). PPy can be electrochemically generated and deposited on the conducting surfaces *i.e.* by electropolymerization. This technique is successfully applied for development of various types of electrochemical sensors and biosensors (Ramanavicius *et al.*, 2006). PPy obtains from electropolymerization of pyrrole monomer as shown in Figure 2.2.

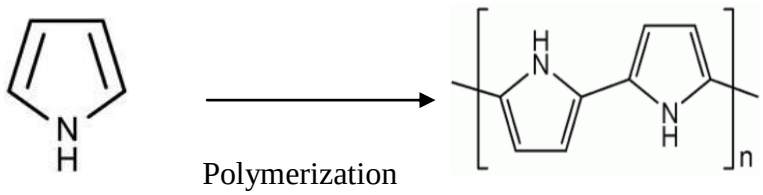

Pyrrole monomer Polypyrrole

Figure 2.2: Polymerization of pyrrole monomer to polypyrrole.

The electropolymerization technique involving direct formation of conducting polymer onto the device of interest and this method was applied for the nitrate electrochemical sensor. The discussion on the electropolymerization process of PPy on carbon electrode surface will be further discussed in Chapter 3 later. Upon completion of the polymerization process, nitrate sensor membrane will be dispensed on the same carbon surface.

CHAPTER 3

EXPERIMENTAL

This chapter gives a full list of chemicals and reagents to be used in conducting the research. The brand of the chemicals and reagents used are also given alongside the materials. Also under this chapter, brief explanations of the synthesis procedure and characterization steps taken are also given.

3.1 Chemicals and reagents

a. Carbon paste, Electrodag from Henkel

b. Carbon paste, Jujo from Jelcon

c. Potassium chloride, KCl from Merck

d. Tetraoctylammonium nitrate, TOAN from Fluka

e. Poly(vinyl chloride), PVC from Fluka

f. Nitrophenyl octyl ether, NPOE from Fluka

g. Tetrahydrofuran**,** THF from Merck

h. Pyrrole from Fluka

i. Potassium nitrate, KNO_3 from Sigma-Aldrich

j. Methyl methacrylate, MMA from Sigma-Aldrich

k. *n*-butyl acrylate, nBA from Sigma-Aldrich

l. Benzene from Merck

m. Benzoyl peroxide from Merck

n. Deionized water, DI water

Table 3.1: Types of prepared solutions.

Solutions	Concentration required
Potassium chloride, KCl	0.1 M
Pyrrole	0.1 M
Nitrate test solution; potassium nitrate, KNO_3	$1X10^{-1}$ M, $1X10^{-2}$ M, $1X10^{-3}$ M, $1X10^{-4}$ M, $1X10^{-5}$ M, $1X10^{-6}$ M, $1X10^{-7}$ M,$1X10^{-8}$ M, $1X10^{-9}$ M

Concentration of nitrate test solution is usually expressed in logarithm where log concentration of $1X10^{-1}$ M is -1 and log concentration of $1X10^{-3}$ M is -3 and so on. In this study -9 (log concentration of $1X10^{-9}$ M) to -1 (log concentration of $1X10^{-1}$ M) will be used.

3.2 Equipments

a. AUTOLab Potentiostat with Metrohm Ag/AgCl double junction reference electrode and platinum counter electrode

b. Thermo Orion ion meter and Orion Ag/AgCl double junction reference electrode

c. Analytical balance

d. Ultrasonic bath 50 Hz by Fischer Scientific

e. Newlong screen print with stencil

f. Olympus high magnification microscope, with magnification 200x

g. Protech water bath

h. Binder oven

j. Protech temperature controlled water bath

3.3 Apparatus

a. Micropipette, 1000 µL

b. Micropipette, 100 µL

c. Micropipette, 10 µL

d. Spatula

e. Glass bottle, 5 ml

f. Volumetric flask 100 ml

g. Glass bottle, 25 ml

h. Thermometer

3.4 Nitrate sensor fabrication process flow

This segment describes the fabrication steps for nitrate sensor starting from PCB material. Fabrication steps are depicted in flowchart as stated in Figure 3.1.

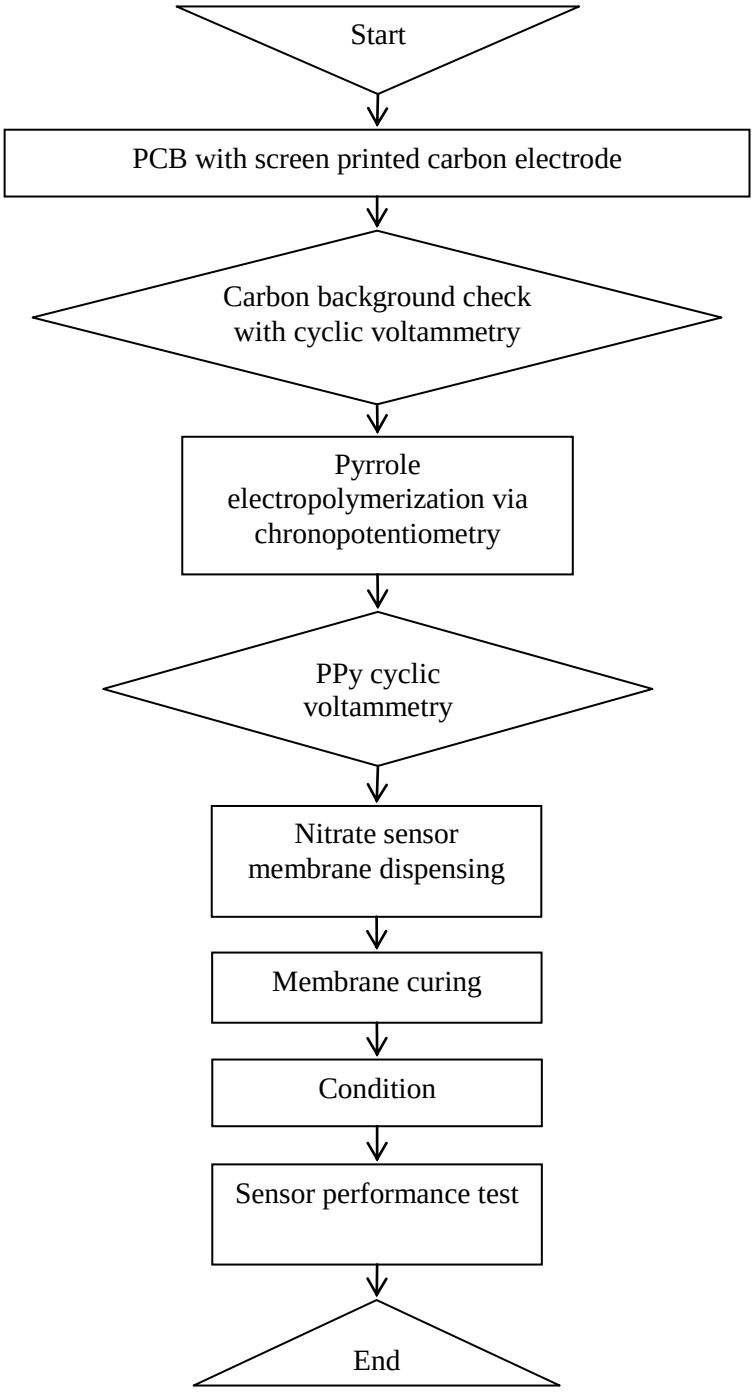

Figure 3.1: Fabrication steps for nitrate sensor.

3.4.1 Electrode characterization

PCB with and without silver (Ag) layer were used to characterize the carbon electrode. Carbon electrodes used were Electrodag (ED) from Henkel and Jujo (J) from Jelcon. Electrode experimental setups were as below:

i. Electrodag carbon paste on PCB with Ag layer

ii. Jujo carbon paste on PCB without Ag layer

iii. Electrodag carbon paste on PCB without Ag layer

iv. Electrodag and Jujo carbon pastes on PCB without Ag layer

Carbon pastes were screen printed on PCB using stencil opening of 4 mm diameter and 100 µm thickness to create a uniform carbon layer. Carbon layer on the PCB will have thickness between 80 to 100 µm. As PCB with carbon paste were then cured in oven at 80 °C for 30 minutes for Electrodag and 120 °C for 15 minutes for Jujo carbon paste. Characterization was performed for each setup above. Electrode *i.e.* working electrode (WE) were characterized with potentiostat (AUTOLab), with potentiostatic program controlled by using Nova 1.8 software. Characterization was performed with cyclic voltammetry set up and experiment was done at room temperature (25 °C). WE, platinum counter electrode (CE) and Metrohm Ag/AgCl double junction reference electrode were immersed into 0.1 M KCl solution. Scanning voltage potential was set up at 1 V for upper value and -1 V for lower value with scan rate of 0.1 V/sec.

3.4.2 Pyrrole electropolymerization

Electrpolymerization was carried out with potentiostat (AUTOLab) with galvanostatic program controlled by using Nova 1.8 software. Polymerization was performed with chronopotentiometry set up and experiment was done at room temperature (25 °C). CE,

WE and Metrohm Ag/AgCl double junction reference electrode were immersed into a mix of 0.1 M KCl and pyrrole 0.1 M. Current 2.5 mA was applied on WE for 90 seconds to allow deposition of PPy.

3.4.3 Polypyrrole (PPy) characterization

Polypyrrole, PPy was characterized with potentiostat (AUTOLab), with potentiostatic program controlled by using Nova 1.8 software. Characterization was performed with cyclic voltammetry set up and experiment was done at room temperature (25 °C). CE, WE and and Metrohm Ag/AgCl double junction reference electrode were immersed into KCl 0.1 M. Scanning voltage potential was performed from -0.1 V to 0.4 V *vs*. Ag/AgCl with scan rate of 0.1 V/second.

3.4.4 Membrane preparation

3 mg of tetraoctylammonium nitrate (TOAN) was weight and mix with 3.3 mg of MB28 glue. MB28 was prepared using mixture of 2 parts of methyl methacrylate (MMA) with 8 parts of *n*-butyl acrylate (nBA). Next, 29.7 mg of PVC and 64.4 µL of nitrophenyl octyl ether (NPOE) were added into the mixture. 1 ml of tetrahydrofuran (THF) was added into the bottle. The membrane mixture was shaken and left in the ultrasonic bath until it was diluted and homogenized. The glass bottle was closed with the cap and was sealed around with parafilm to avoid evaporation. The membrane cocktail was then kept in refrigerator for cool storage of below 4 °C.

3.4.5 Membrane dispensing and curing

A total of 30 µL of membrane cocktail (5 dispenses x 6 µL per portion) was dispensed on the carbon surface. The separate dispensing in few smaller amounts is to allow uniform spreading of the membrane on the carbon surface and avoiding overflow. Once dispensing completed the sensor with PVC based membrane was cured with low flow rate of nitrogen gas for 1 hour and was left at room temperature overnight for complete curing.

3.4.6 Membrane condition

Membrane was conditioned in idle with 0.1 M KNO_3 for minimum of 1 hour before perform any testing. Condition prepares the mobility of the ion exchanger which initially dry and static in membrane site to achieve fast and stable reading during measurement.

3.5 Nitrate sensor performance test process flow

This segment describes the tests to be performed on nitrate sensor. Tests are defined as per flowchart in Figure 3.2.

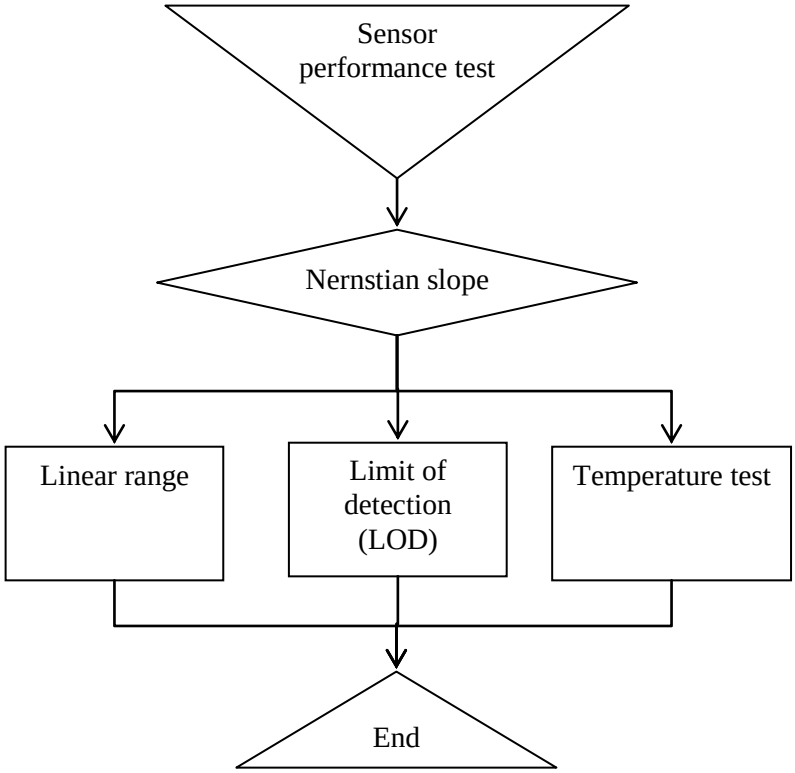

Figure 3.2: Test flow for nitrate sensor.

3.5.1 Ion selective electrode (ISE) Nernstian slope test

Slope test was performed by using test solutions of 1 X 10^{-1} M, 1 X 10^{-2} M, 1 X 10^{-3} M, and 1 X 10^{-4} M KNO_3. Fabricated ISE sensor and Orion Ag/AgCl double junction reference electrode were connected to the Thermo Orion ion meter as in Figure 3.3. Measurements were performed by dipping the sensor and reference electrode in the KNO_3 solutions starting from the lowest concentration 1 X 10^{-4} M (log concentration = -4) to the highest concentration 1 X 10^{-1} M (log concentration = -1) of KNO_3.

Figure 3.3: Measurement setup for ion-selective electrode potentiometric cell.

3.5.2 Linear range and limit of detection, LOD

The same measurement method was performed as the ISE Nernstian slope in 3.5.1. Linear range and limit of detection require test to be performed starting from 1 X 10^{-9} M (-9) to 1 X 10^{-1} M (-1) of KNO_3.

3.5.3 Temperature test

Test solution with concentration of 1 X 10^{-1} M, 1 X 10^{-2} M, 1 X 10^{-3} M, and 1 X 10^{-4} M KNO_3 M were placed into the water bath to be chilled to 10 °C and also heated to 50 °C to observe the calibration curves or slope values at these temperatures. Fabricated ISE sensor and Orion Ag/AgCl double junction reference electrode were connected to the Thermo Orion meter while the test solution in the glass bottle was immersed in the water bath with specified temperature. Measurements were performed by dipping the sensor and reference electrode in the KNO_3 solutions starting from the lowest concentration 1 X 10^{-4} M (log concentration = -4) to the highest concentration 1 X 10^{-1} M (log concentration = -1) of KNO_3.

CHAPTER 4

RESULTS AND DISCUSSIONS

This chapter gives full results of the experimental from the methods described in Chapter 3 with complete explanations.

4.1 Carbon electrode observations

Oven cured carbon screen printed on PCB (with and without Ag layer) were inspected under high magnification microscope for appearance check. Ag on the PCB act as a conductor layer in order to have a good contact with copper (Cu) track in the polyethylene (PET) layer of the PCB. Figure 4.1 shows all four wells of the PCB; well 1 (W1), well 2 (W2), well 3 (W3) and well 4 (W4) were covered with carbon *via* screen printing process and oven cured.

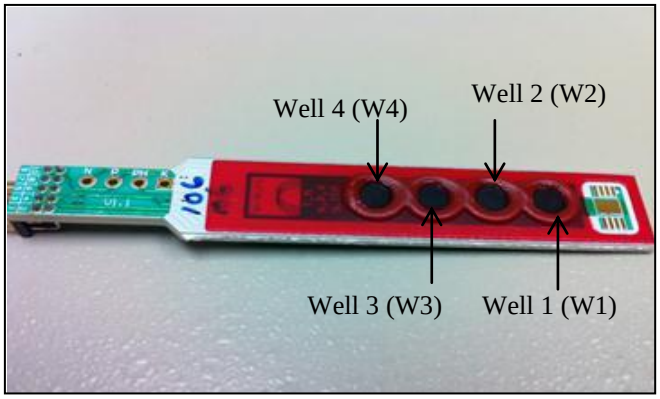

Figure 4.1: PCB element with wells covered with cured carbon (with and without Ag).

The construction of the nitrate sensor is shown in Figure 4.2; example shown below is with Ag layer.

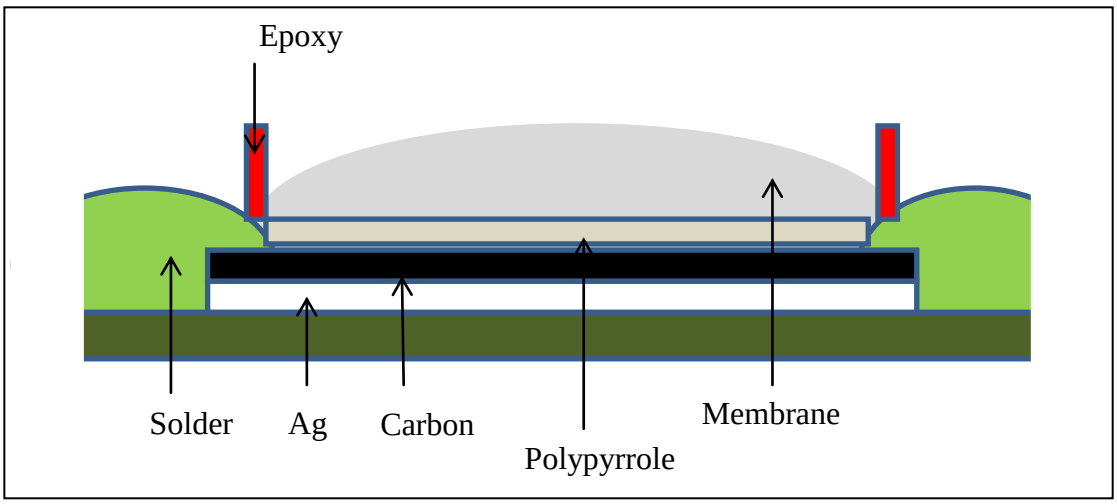

Figure 4.2: The construction of the nitrate sensor.

The details of the nitrate sensor construction will be discussed in section 4.2 to 4.4. Figure 4.3 shows one of the well from PCB with Ag and Electrodag carbon layer. Few spots of exposed Ag were detected. The results were compared with PCB without Ag, where no exposed carbon layer detected. Electrodag carbon has good adhesion to plastic and paper substrates as indicated in the Electrodag Technical Data Sheet thus it provides uniform spread on top of the PET layer. It is proven in Figure 4.4 where there is no exposed Ag observed under high magnification scope. This is due to suitability of Electrodag carbon paste for printing on plastic layer which resulted a smooth and uniform printing on the PET layer with excellent coverage compare to Ag layer.

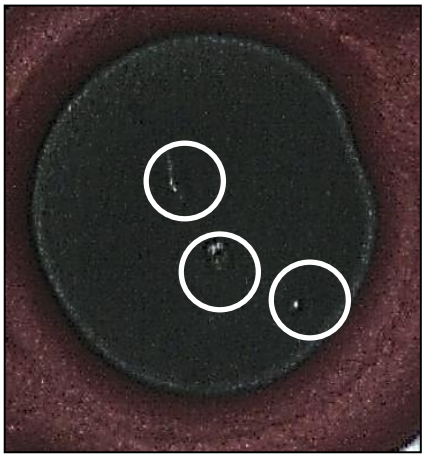

Figure 4.3: Exposed Ag on PCB (with Ag) and Electrodag carbon layer.

It is very important to achieve a fully covered carbon surface on PCB as the exposed Ag will interact with chloride (Cl^-) from 0.1 M KCl electrolye and produce silver chloride (AgCl) salt during PPy growing process on carbon layer. AgCl white crystal salt will form on the exposed area and this will reduce the surface area for the nitrate membrane contact.

$$Ag^+_{(s)} + Cl^-_{(l)} \longrightarrow AgCl_{(s)} \qquad \text{[Equation 4.1]}$$

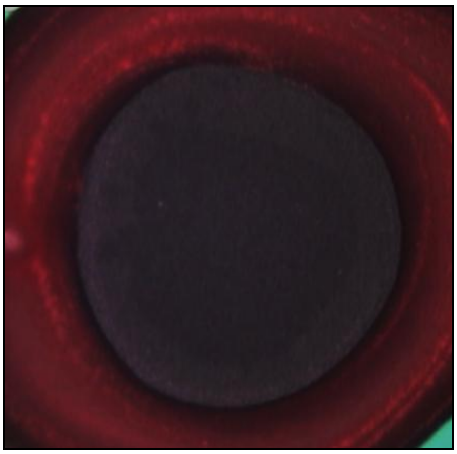

Figure 4.4: Electrodag carbon layer on PCB PET (without Ag)

4.2 Carbon electrode characterization

4.2.1. Electrodag carbon paste on PCB with Ag layer

Electrodag carbon paste has low resistivity *i.e.* less than 30 Ohms/cm^2 a high conductivity which suitable for printing on plastic layer (substrate) in sensor fabrication. It consists of up to 60% of methyl isobutyl ketone, 30% of graphite resulted high conductivity, 10% of carbon black and 1% of silica (all components % are by weight). Methyl isobutyl ketone acted as low viscosity solvent which helps in screen printing process to produce uniform carbon layer as shown in Figure 4.4. Figure 4.5 shows cyclic voltammogram of Electrodag carbon at W1, W2 and W3 directly on PCB plastic layer without Ag layer. Carbon peaks were observed during oxidation at 0.1 V *vs.* Ag/AgCl and peak current is 0.0015 mA. No carbon peak was observed during reduction process.

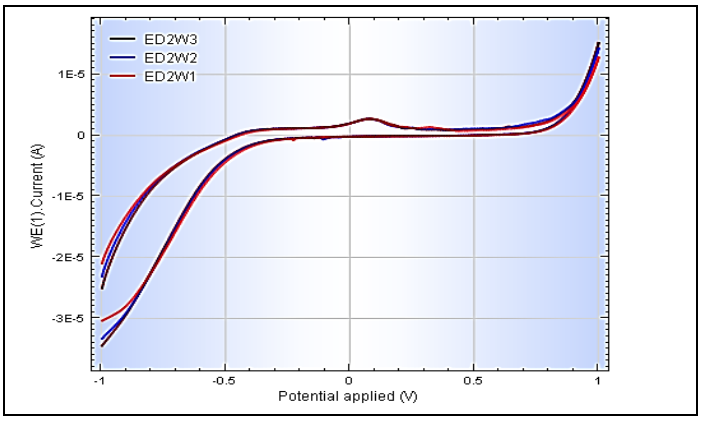

Figure 4.5: Cyclic voltammogram of Electrodag carbon paste on PCB with Ag layer.

4.2.2 Jujo carbon paste on PCB without Ag layer

Jujo (J) carbon paste has lower resistivity compare to Electrodag. *i.e*. 10 ohms/cm^2, and it shares high conductivity and good printability. It is suitable for membrane and for printing on poly(ethylene terephthalate) (PET) substrate. It consists of up to 30% of diethyleneglycol monoethylether acetate, 15% of aromatic hydrocarbon (petroleum

naphtha), 25% of synthetic resin, 25% pigment and 10% of carbon black (all components % are varied by weight). Jujo provides homogenous and uniform carbon pasted layer. Figure 4.6 shows cyclic voltammogram for Jujo carbon at W1, W2 and W3. Carbon peaks were observed during oxidation at 0.1 V *vs*. Ag/AgCl and peak current is 0.0015 mA. No carbon peak was observed during the cathodic scan. Results are similar with Electrodag carbon paste on PCB with Ag layer..

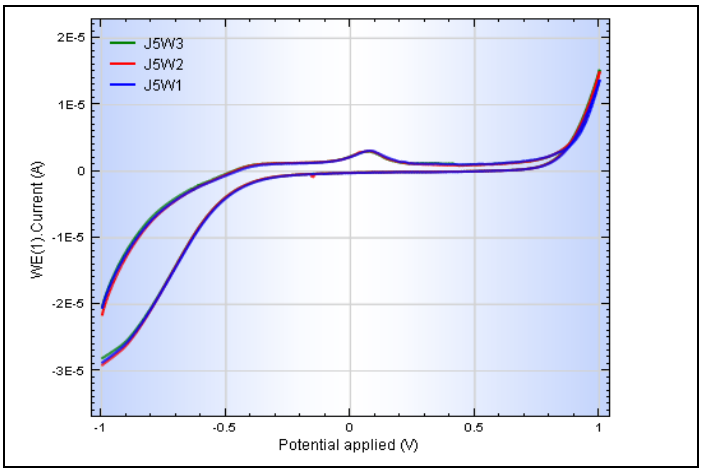

Figure 4.6: Cyclic voltammogram of Jujo carbon paste on PCB without Ag layer.

4.2.3 Electrodag carbon paste on PCB without Ag layer

Ag has high conductivity and its function is to provide high electric conductivity between Cu circuit (in plastic layer) of the PCB and carbon pastes. Electrodag was chosen to be used in this experiment as it provides good adhesion with plastic surface. Figure 4.7 shows cyclic voltammogram for Electrodag carbon on Ag layer at W1, W2 and W3. Carbon peaks were observed during oxidation at 0.1 V *vs*. Ag/AgCl and peak current is 0.002 mA. There is no carbon peak on the cathodic scan range. Results are similar with Electrodag carbon paste on PCB without Ag layer.

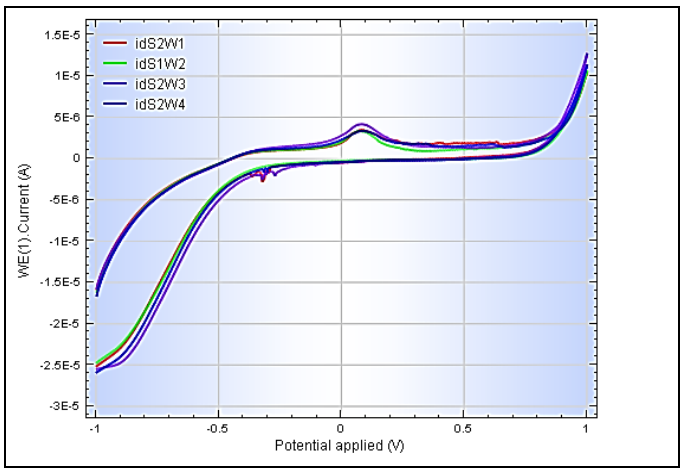

Figure 4.7: Cyclic voltammogram of Electrodag carbon paste on PCB without Ag layer.

4.2.4 Electrodag and Jujo carbon pastes on PCB without Ag layer

Electrodag (ED) and Jujo (J) carbon paste were both printed on the same PCB without Ag layer. Electodag printed on top of the PCB followed by Jujo. Electrodag was chosen as the first carbon paste layer on PET as it is suitable to be printed on any plastic surface whereas Jujo is selected as the second carbon layer due to its suitability for the membrane adhesion and has lower resistance compare to carbon paste from Electrodag. Figure 4.8 shows cyclic voltammogram for both Electrodag and Jujo carbon at W1, W2 and W3. Carbon peaks were observed during oxidation at 0.1 V *vs*. Ag/AgCl and peak current is 0.0055 mA. No carbon peak was observed during the reduction scanning. Results are similar with Electrodag carbon paste on PCB without Ag layer. Peak current is expected to be higher compared to PCB with single layer of carbon as two carbon layers resulted in better oxidation process.

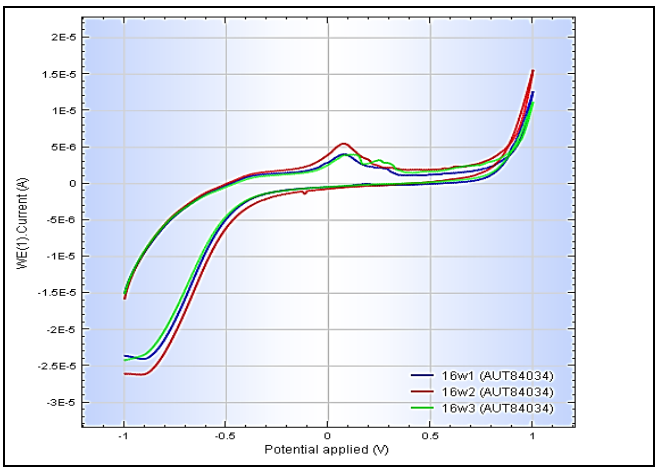

Figure 4.8: Cyclic voltammogram of Electrodag and Jujo carbon pastes on PCB without Ag layer.

Figure 4.9 shows SEM of the cross-section of PCB with two carbon layers (Electrodag and Jujo). Total cured printed carbon thickness is 99.4 µm. Good coverage of these carbon pastes were observed on top of PCB layer with no exposed area.

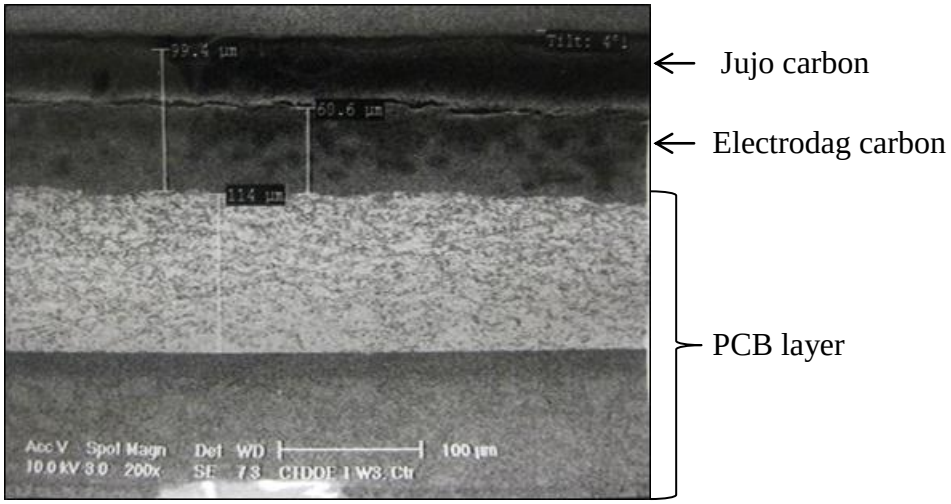

Figure 4.9: Electrodag and Jujo carbon layers on top of PCB

It is noticeable that the thickness of coverage by Jujo carbon is about half lesser than Electrodag carbon. This can be explained in terms of resistivity where it is much harder for carbon paste from Jujo to be deposited on Electrodag surface compare to deposition

of Electrodag carbon on the surface of PCB due to the higher resistivity possess by Electrodag carbon itself.

4.3 Pyrrole chronopotentiometry

Chronopotentiometry profile for each setups are shown in Figure 4.10 to Figure 4.13. The electrochemical behavior of each setup will be discussed in Section 4.4 with results provided from cyclic voltammetry of PPy forms during chronopotentiometry setup.

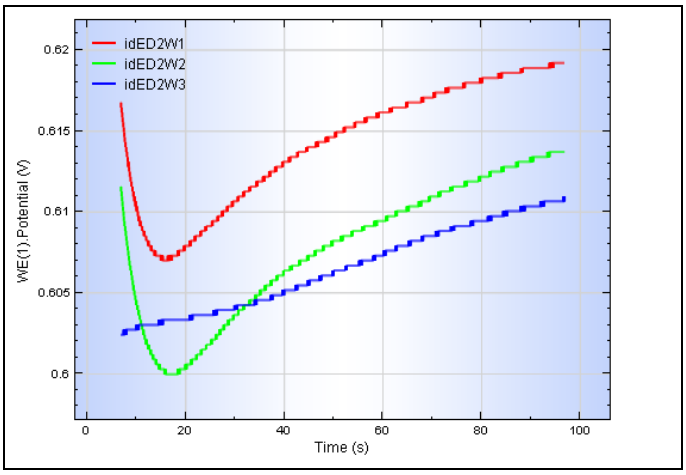

Figure 4.10: Chronopotentiometry profile of Electrodag carbon paste on PCB with Ag layer.

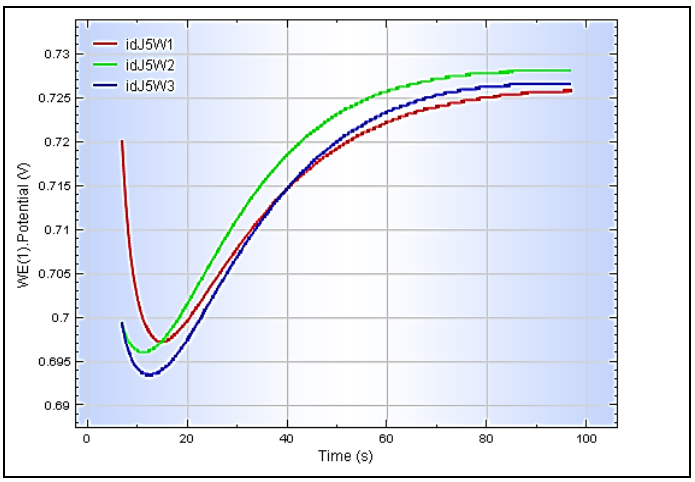

Figure 4.11: Chronopotentiometry profile of Jujo carbon paste on PCB without Ag layer.

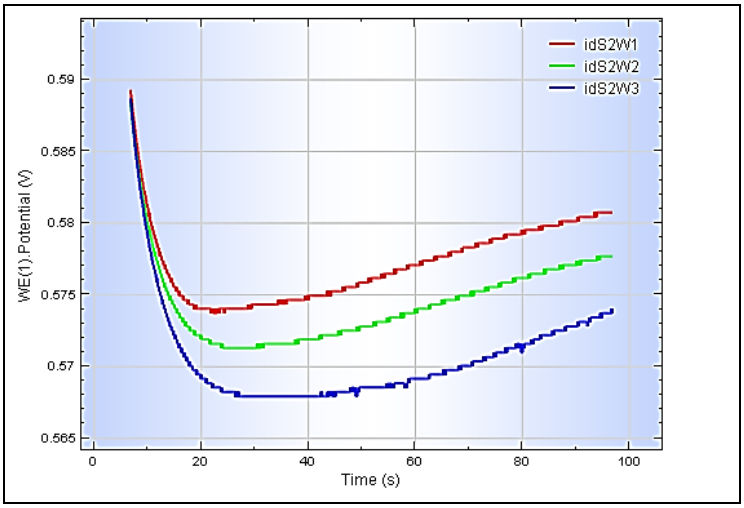

Figure 4.12: Chronopotentiometry profile of Electrodag carbon paste on PCB without Ag layer.

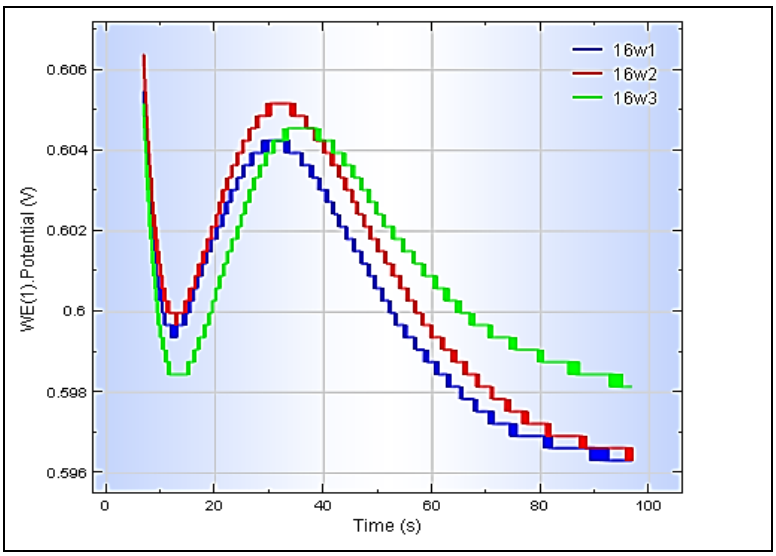

Figure 4.13: Chronopotentiometry profile of Electrodag and Jujo carbon pastes on PCB without Ag layer.

4.4 Polypyrrole cyclic voltammetry

4.4.1 Electrodag carbon paste on PCB with Ag layer

Figure 4.14 shows the cyclic voltammogram of PPy film on the Electrodag carbon electrode (PCB without Ag layer). Pyrrole oxidation is clearly observed as an anodic peak for all three carbon wells with peak current at 0.10 V *vs*. Ag/AgCl, that represents to the signature of PPy oxidation. It indicates the formation of the oxidized state of PPy deposited on the Electrodag carbon electrode during the cycle. The pyrrole reduction occurs between -0.6 V to -1.0 V *vs*. Ag/AgCl. Pyrrole reduction peak is observed at between -0.8 V to 0.9 V *vs.* Ag/AgCl for all three wells.

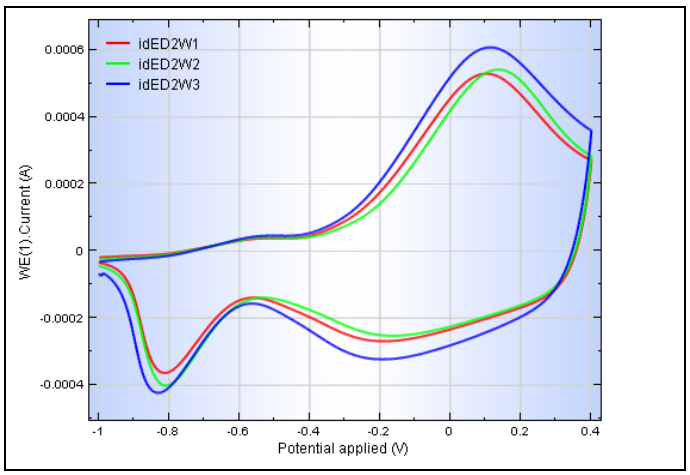

Figure 4.14: Cyclic voltammogram of Electrodag carbon paste on PCB with Ag layer.

4.4.2 Jujo carbon paste on PCB without Ag layer

Figure 4.15 shows the potentiometry of pyrrole electropolymerized at Jujo carbon electrode (PCB without Ag layer). Pyrrole oxidation is clearly observed as an anodic peak at between 0.10 V to 0.2 V for all three wells. The constant growth of a broad anodic curve is observed between -0.4 V to 0.4 V with peak height of 0.2 mA. The peak's broad and height for PCB electrode with Jujo carbon paste are less compare to electrode with Electrodag carbon paste as depicted in Figure 4.14. The pyrrole reduction occurs between -0.4 V to -1 V with PPy reduction peak observed between -0.65 to -0.7 V *vs*. Ag/AgCl for all three wells.

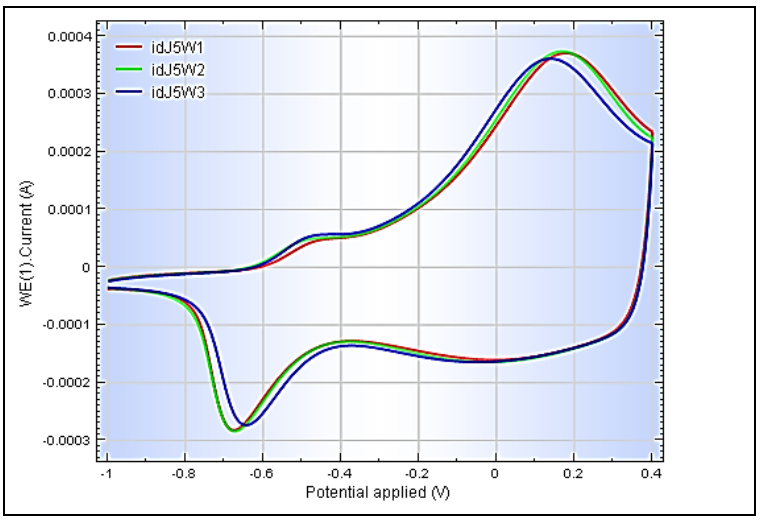

Figure 4.15: Cyclic voltammogram of Jujo carbon paste on PCB without Ag layer.

4.4.3 Electrodag carbon paste on PCB without Ag layer

Figure 4.16 shows the cyclic voltammetry of PPy formed via electropolymerization process on the Electrodag carbon electrode (PCB with Ag layer). The oxidation peak of PPy is observed between 0.1 V to 0.2 V, referenced to Ag/AgCl for all three carbon wells. The oxidation curve width is observed from -0.4 V to 0.4 V (*vs*. Ag/AgCl) with peak height of 0.1 mA. As compared to previous voltammogram (Figure 4.14), the redox oxidation activity of PPy had encountered a large shrinkage. This is most probably due to the exposed Ag layer from the PCB had reacted with the chloride ion from KCl electrolyte; thus forming a thin layer of AgCl on the carbon layer. This in turn reduces the active surface area for the PPy, thus resulting weaker oxidation peak. The PPy still undergoes reduction response between -0.4 V to -1 V *vs*. Ag/AgCl, with the maximum cathodic peak at -0.7 V to -0.75 V *vs*. Ag/AgCl for all three PPy films on different wells.

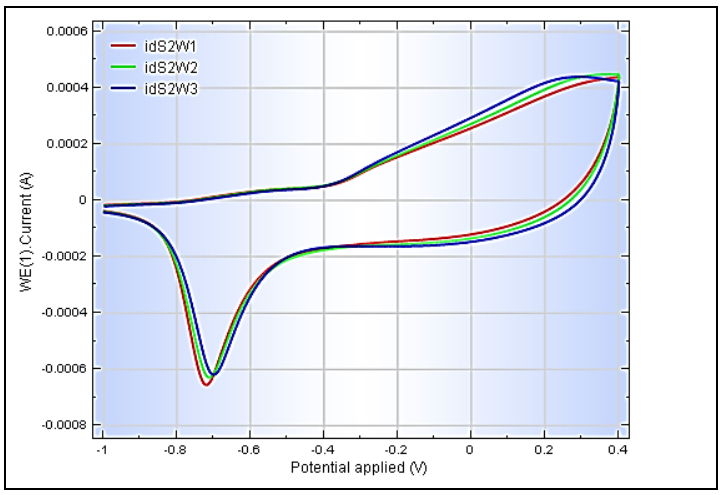

Figure 4.16: Cyclic voltammogram of Electrodag carbon paste on PCB without Ag layer.

4.4.4 Electrodag and Jujo carbon pastes on PCB without Ag layer

Figure 4.17 shows the voltammogram of pyrrole electropolymerized on PCB electrode modified with Electrodag and Jujo carbon electrode pastes. Distinctive PPy oxidation peak is clearly observed at 0.05 V to 0.1 V *vs.* Ag/AgCl for all three wells. The polypyrrole oxidation curve is between -0.4 V to 0.4 V, referenced to Ag/AgCl with peak current of 0.43 mA. This indicates the PPy film is successfully deposited on the Electrodag and Jujo carbon electrode during the chronopotentiometry. The PPy reduction occurs between -0.6 V to -1.0 V, *vs.* Ag/AgCl. Pyrrole reduction peak is clearly observed at -0.8 V, referenced to Ag/AgCl for all three wells.

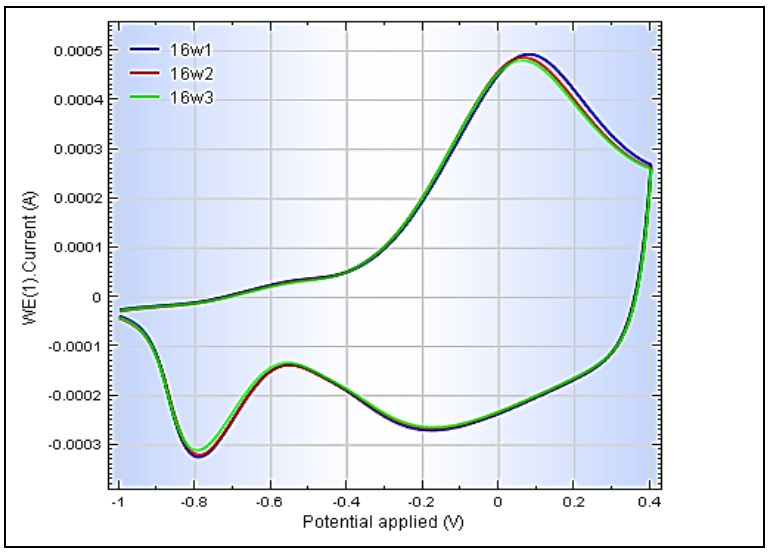

Figure 4.17: Cyclic voltammogram of Electrodag and Jujo carbon pastes on PCB without Ag layer.

Table 4.1: Cyclic voltammogram data comparison between four types of electrode.

	Anodic peak range	Cathodic peak range	Anodic peak height
Electrodag carbon paste on PCB with Ag layer	0.1 V to 0.14 V	-0.8 V to 0.9 V	0.40 mA
Jujo carbon paste on PCB without Ag layer	0.1 V to 0.2 V	-0.65 to -0.7 V	0.20 mA
Electrodag carbon paste on PCB without Ag layer	0.1 V to 0.2 V	-0.7 V to -0.75 V	0.10 mA
Electrodag and Jujo carbon pastes on PCB without Ag layer	0.05 V to 0.1 V	-0.6 V to -1.0 V	0.43 mA

All the cyclic voltammogram of PPy observed above shared the similar profile with many studies that have been reported (Woo *et al.*, 2008; Careem *et al.*, 2006 and Porras-Gutierrez *et al.*, 2013). Based on the comparison in Table 4.1, it is clearly shows that carbon electrode comprises of both Electrodag and Jujo on the PCB without Ag layer is the most suitable electrode used for electrochemical sensor. It has the highest sensitivity and robustness as indicated with sharp and distinct PPy peaks in both anodic and cathodic scans and highest anodic peak current compared to single layer carbon electrode and electrode with Ag layer.

4.5 Electrode with nitrate sensor membrane

All four types of electrodes above were to proceed with membrane dispensing and curing process. Figure 4.18 shows the electrode with cured membrane.

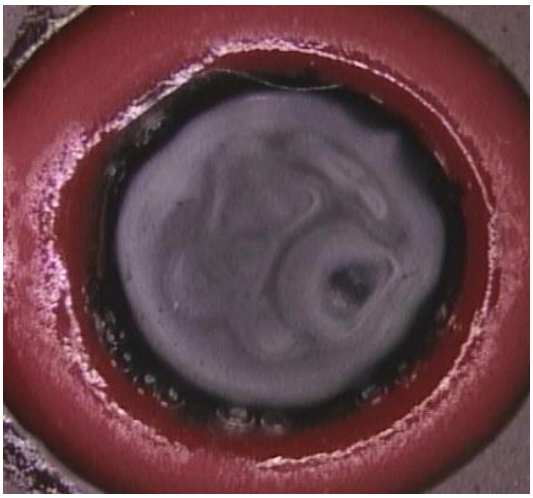

Figure 4.18: Electrode with cured membrane.

The nitrate sensor membrane contains quaternary ammonium salt; tetraoctylammonium nitrate (TOAN) *i.e*. lipophilic additive in polymeric membrane without ionophore as it increases the characteristic selectivity pattern for example the Hofmeister selectivity series. The chemical structure of TOAN is shown in Figure 4.19.

It functions as an ion exchanger in the ISE solid polymeric membrane (Zubrowska *et al.*, 2011). The mechanism is explained in Figure 4.20 later.

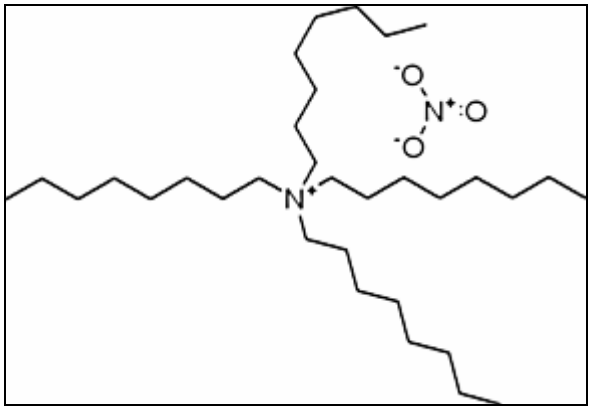

Figure 4.19: TOAN chemical structure.

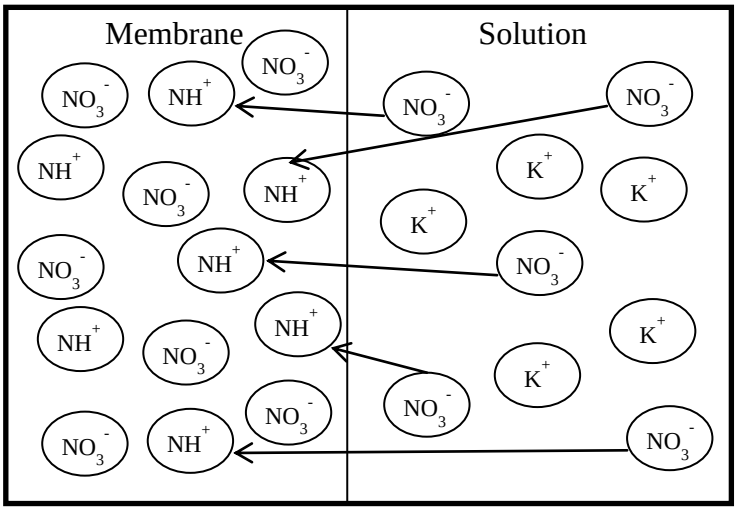

Figure 4.20: Nitrate membrane mechanism.

From the mechanism, the amine ion (NH^+) attracts nitrate ions (NO_3^-) from the solution into membrane layer and also acts as carrier for the nitrate ions (Figure 4.20). The amine with positive surface charge is highly active; thus it attracts and allows nitrate ion adsorbed on its surface. This had resulted higher concentration of nitrate ions in the membrane layer due to migration of nitrate ions from TOAN, compare to the

nitrate concentration in the bulk solution, thus resulted in electrical potential difference. The similar mechanism is also reported by Zubrowska in year 2011.

4.6 Sensor with Nernstian response

The electrodes were conditioned in log concentration of –1 KNO_3 solution for minimum of 1 hour prior testing. ISE sensor Nerstian slopes were obtained from the response value in KNO_3 solution from log concentration of -4 to -1 which constructed as calibration curve. The slope values obtained were referred to the recommended Nernstian ideal slope at 25 °C. The ideal slope value for ISE sensor for nitrate is -59.16 mV/decade (Buck *et.al.*, 1994; Guilbault, 1981). All four types of electrode sensors with membrane were tested to obtain calibration curve and with the aim to achieve Nernstian slope value.

4.6.1 Electrodag carbon paste on PCB with Ag layer

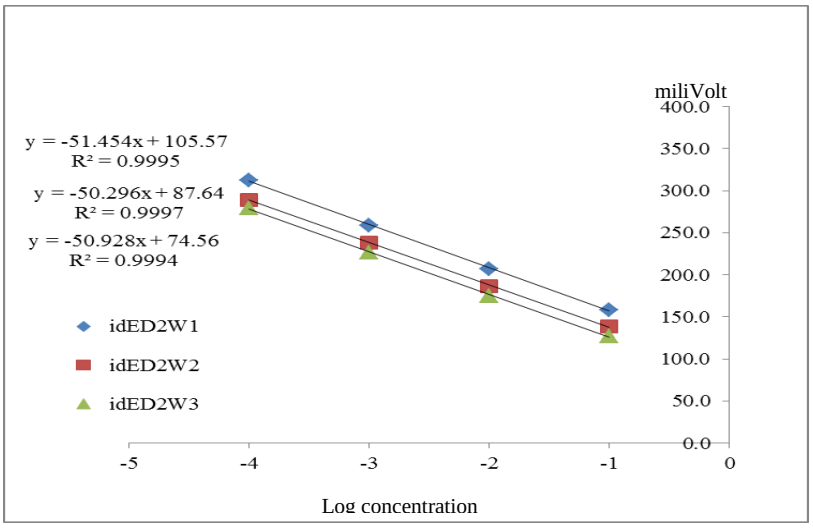

Figure 4.21: ISE slope for Electrodag carbon paste on PCB with Ag layer.

4.6.2 Jujo carbon paste on PCB without Ag layer

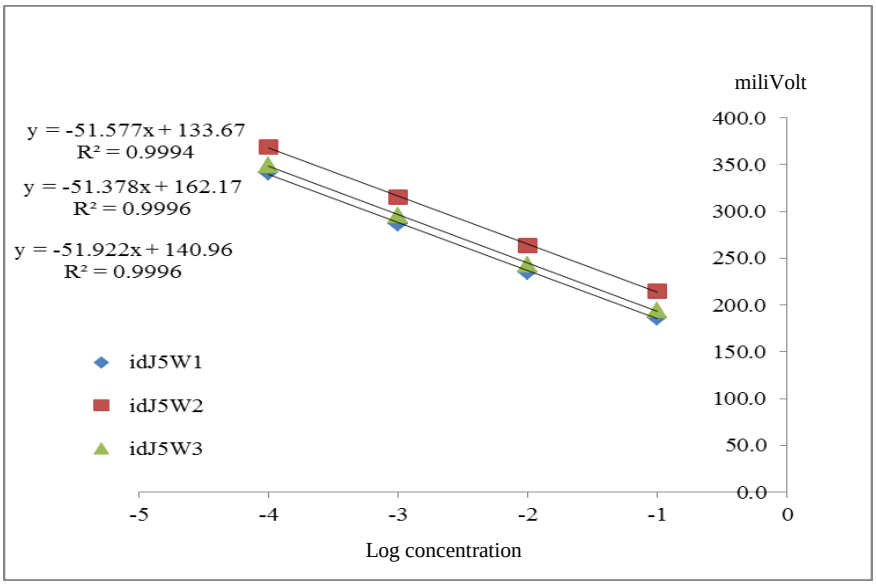

Figure 4.22: ISE slope for Jujo carbon paste on PCB without Ag layer.

4.6.3 Electrodag carbon paste on PCB without Ag layer

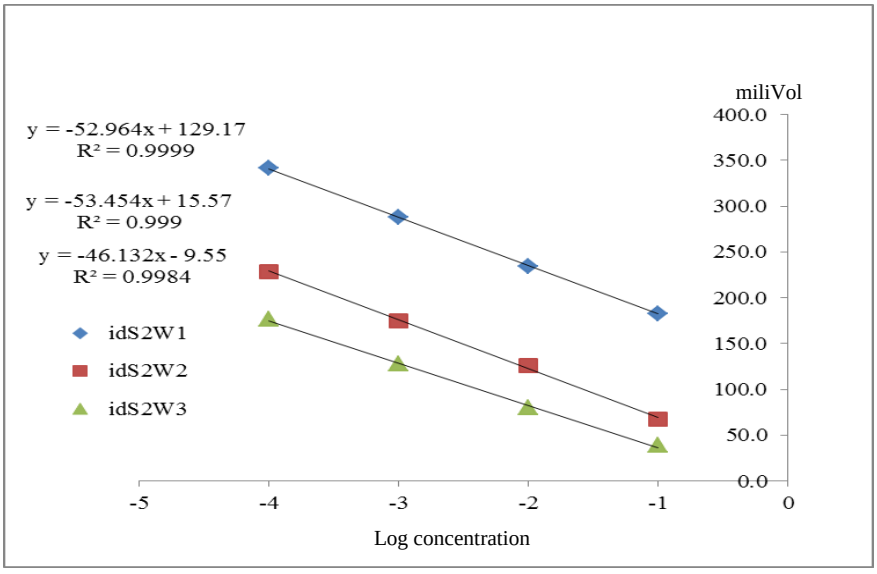

Figure 4.23: ISE slope for Electrodag carbon paste on PCB without Ag layer.

4.6.4 Electrodag and Jujo carbon pastes on PCB without Ag layer

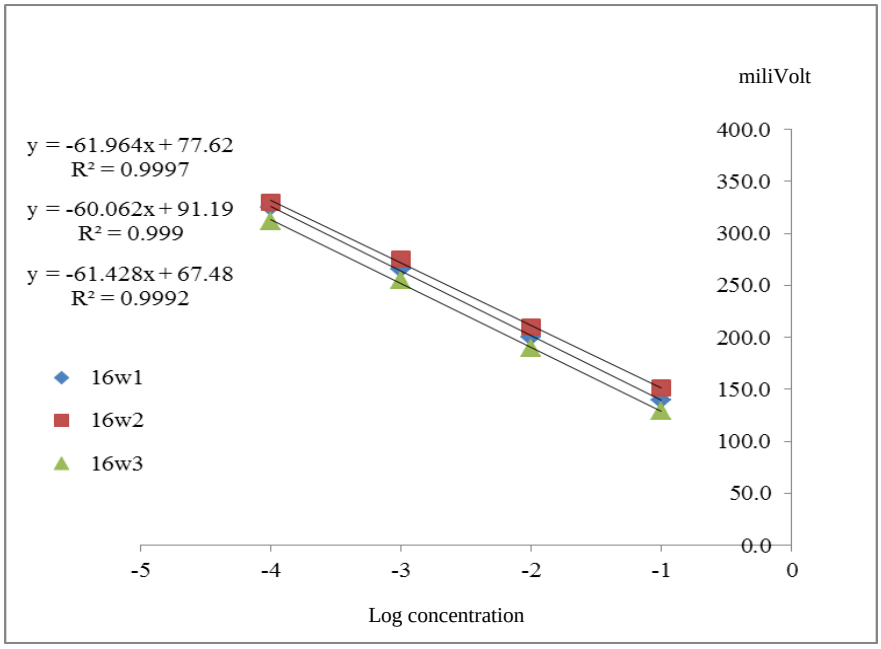

Figure 4.24: ISE slope for Electrodag and Jujo carbon pastes on PCB without Ag layer.

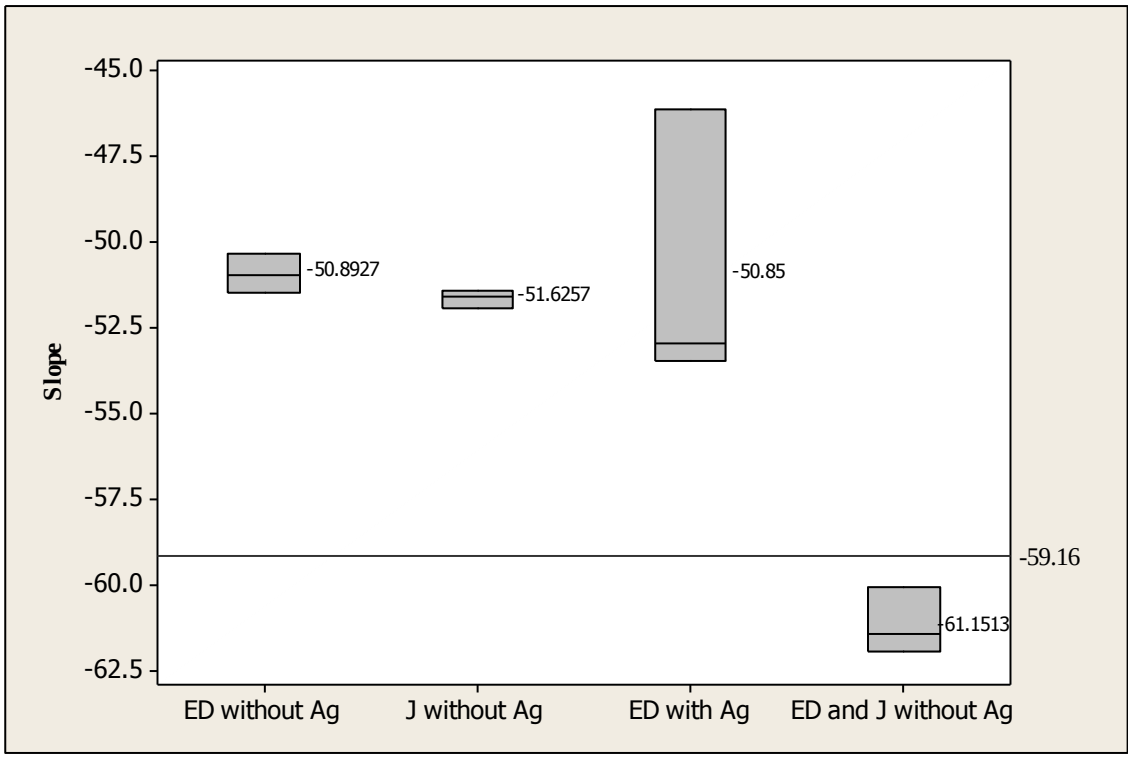

Figure 4.25: Boxplot of all four electrode types with Nernstian slopes values.

ISE with Ag had resulting a wide range of slope values variation as observed in boxplot (Figure 4.25) compared to ISE that tested on sensor membrane without Ag layer. The uncontrollable reaction between Ag from the exposed electrode area with KCl electrolyte during electropolymerization had resulted reduction on surface area for PPy growth. ISE with Ag is found not as sensitive as compared to electrode without Ag layer. The boxplot shows the ISE sensor with Electrodag and Jujo carbon layers (without Ag layer) had the closest slope value to the ideal Nernstian slope for nitrate ions (-59.16 mV/decade) (Buck *et al.*, 1994) compare to all other ISE tested. It indicates that this is the best ISE for determination of nitrate ion.

Slope values observed had indicated the ISE with both Electrodag and Jujo carbon pastes is the most highly sensitive and reliable to detect and quantify nitrate ion concentration in a solution. Linear regression with more than 0.999 is observed for all the ISEs except ISE with Ag layer. This regression value (> 0.999) and above shows response value in mV for each nitrate concentration has a good relationship in producing linear straight line of calibration curve.

4.7 Sensor linear range and limit of detection

ISE sensor with both Electrodag and Jujo carbon layer was then used to determine the lowest concentration of nitrate that can be detected and quantified *i.e.* limit of detection (LOD). The detection limit is defined by the cross-section of the two extrapolated linear parts of the ion-selective calibration curve (Buck *et al.*, 1994). The LOD was obtained from the graph plotted with response measurement in KNO_3 solutions from log concentration of -7 to -1.

Sensor linear range which observed from Figure 4.26 and 4.27 show values are up to log concentration of -5 *i.e.* 1 X 10^{-5} M for both well 1 and well 2. Typically, the electrode calibration curve exhibits linear response range between 10^{-1} M and 10^{-5} M (LOD are at log concentration of -6.3 *i.e.* 5.0X10^{-7} M and log concentration of -6.2 *i.e.* 6.3 X 10^{-7} M for both well 1 and well 2 respectively.

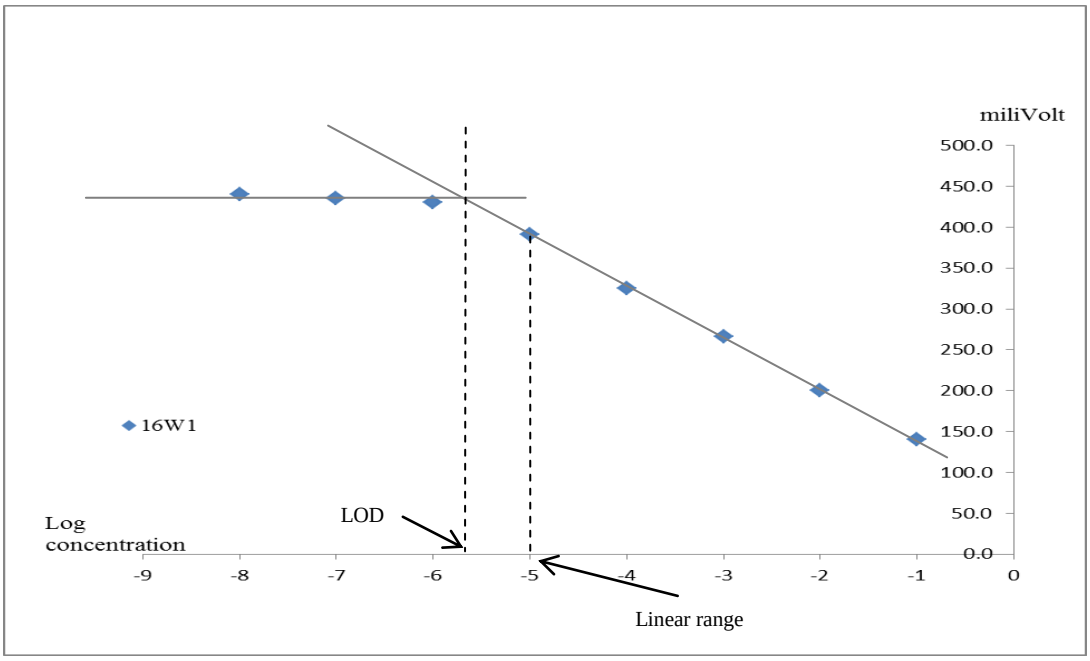

Figure 4.26: Nitrate sensor linear range and LOD for well 1.

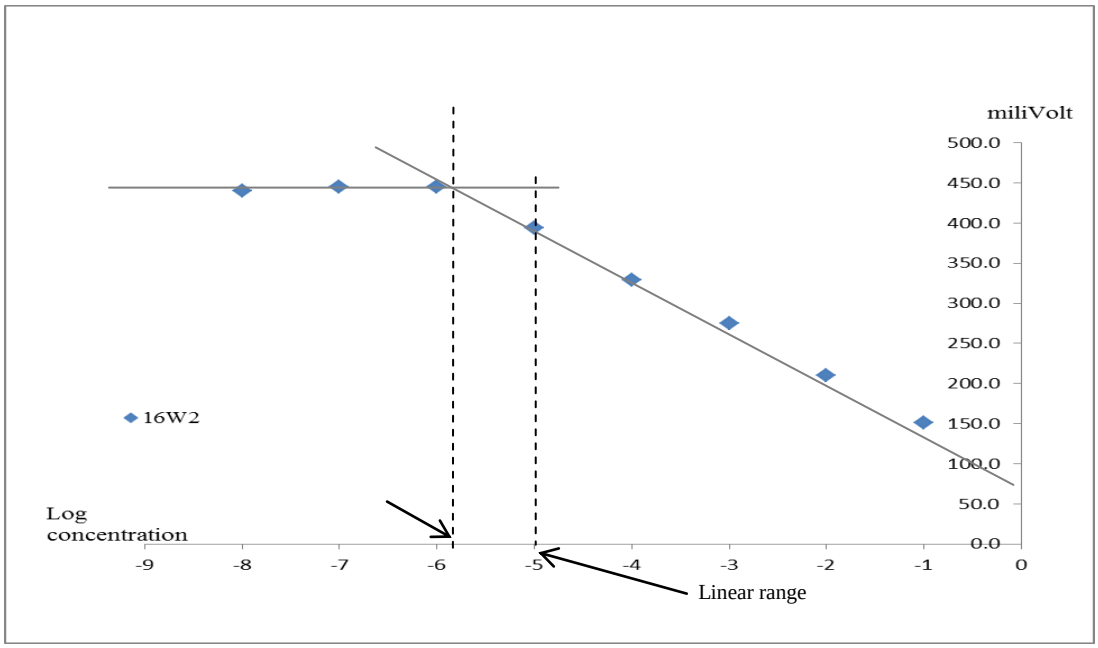

Figure 4.27: Nitrate sensor linear range and LOD for well 2.

4.8 Sensor temperature test

ISE sensor Nerstian slopes were obtained from the response value in KNO_3 solution from log concentration of -4 to -1 in test solution with temperature of 5 °C and 50 °C.

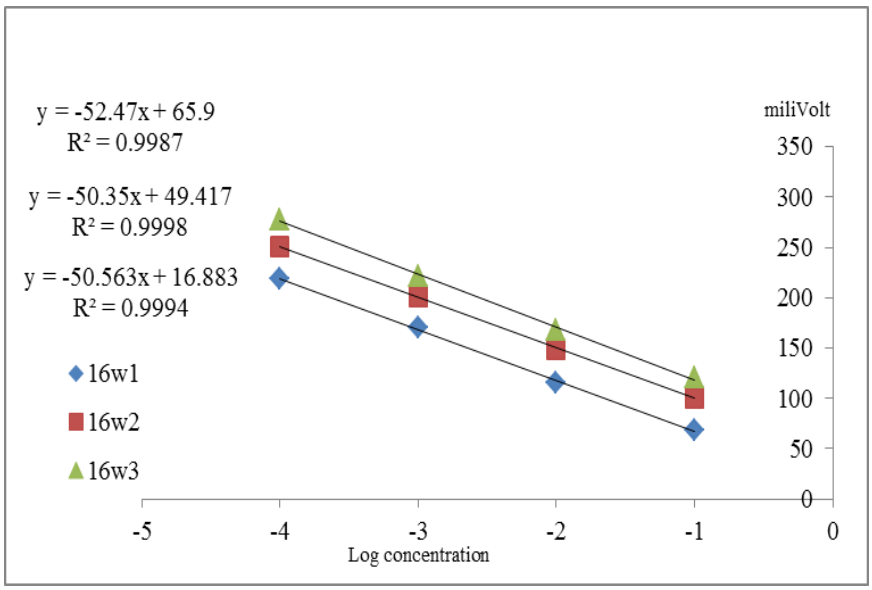

Figure 4.28: Nitrate sensor Nernstian response at 10 °C.

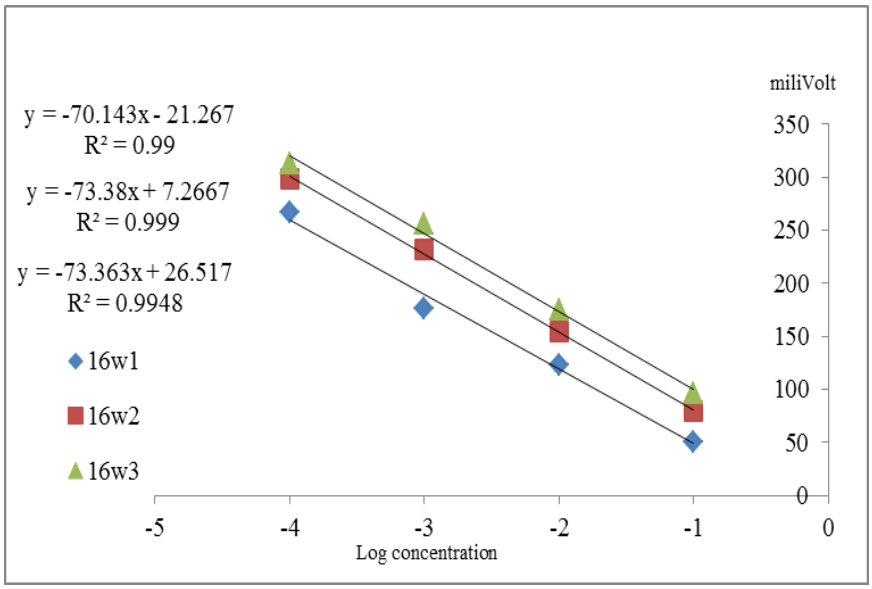

Figure 4.29: Nitrate sensor Nernstian response at 50 °C.

The recommended Nernstian ideal slope at 25°C for nitrate is -59.16 mV/decade (Buck *et al.*, 1994; Guilbault, 1981). Decreased of slope value is observed at 10 °C (refer to Figure 4.28) compare to test performed at 25 °C (refer to Figure 4.24). When higher temperature of test solution was used *i.e.* at 50 °C, higher slope was observed which was about 10mV/decade higher than the ideal Nernstian value for nitrate causing super Nernstian response. The decrease and increase of the Nernstian slope is based on the Nernst equation below whereby slope value is inversely proportional to the temperature.

$$E_{cell} = E^{0}_{Ag/AgCl} + (2.303RT/zF)(\log a) \qquad \text{[Equation 4.2]}$$

Figure 4.30 shows the trend of slope with the rise of the temperature. It is observed from the slope value that approximately -10.58 mV/decade of slope drop for every 1 °C of temperature increase.

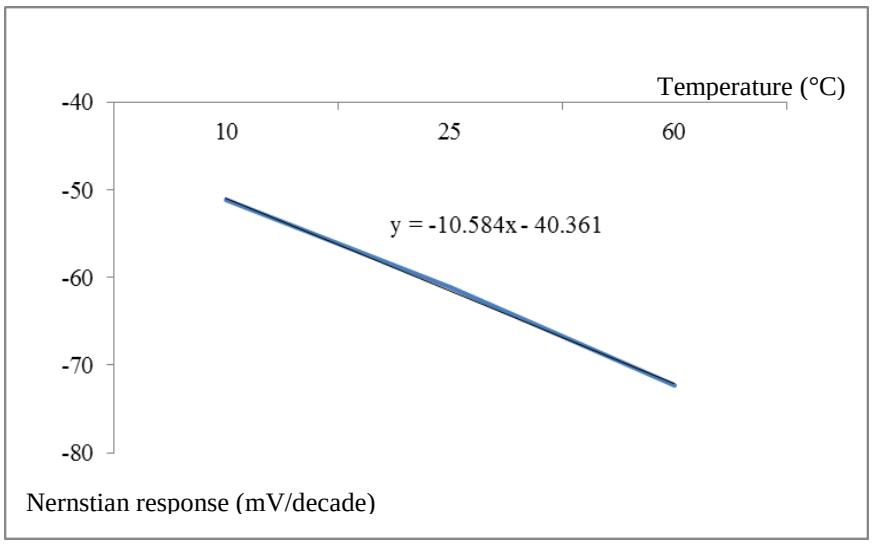

Figure 4.30: Nitrate sensor Nernstian response *vs.* temperature.

CHAPTER 5

CONCLUSION AND RECOMMENDATION

5.1 Conclusion and recommendation

In this research, the development of nitrate ISE sensor was conducted. Four types of electrodes studies were performed on characterizing and identifying the best electrode for nitrate ISE sensor. The electrodes were constructed using PCB with two types of carbon pastes. These electrodes were then undergo surface modification using conducting polymer *i.e.* polypyrrole. The pyrrole was electropolymerized to PPy on top of carbon paste. The next step was dispensing of PVC based ion-selective membrane for nitrate ion and curing process. Prior testing, the electrodes that act as ISE sensors were conditioned in -1 M KNO_3 solution for minimum of 1 hour.

Nernstian slope was obtained from the calibration curve of each electrode. Based on the results, electrode with Ag layer yielded a huge slope variation *i.e.* from -46.13 mV/decade to -53.454 mv/decade. It had shown unreliable slope value for this electrode type and less suitable to be used as ISE sensor. Electrodes without Ag layer had produced stable slope with small variation. Single carbon layer electrode tested *i.e.* with Electrodag carbon has an average slope value of -51.26 mV/decade. The value was still not close to the ideal Nernstian slope *i.e.* -59.16 mV/decade.

The construction of ISE sensor with two carbon layer (Electrodag and Jujo) has improved the slope value to an average value of -61.15 mV/decade with small variation. The combination properties of the carbon used *e.g.* high conductivity, low resistance, provide good adhesion to plastic surface and suitable to be used with membrane contributed to the improvement. Based on the results obtained, it had proven that this type of electrode produce high sensitivity ISE sensor and reliable.

Linear range and limit of detection (LOD) were measured using ISE sensor with double layer carbon. The performance was comparable with all other available ISE in the market. The linear range value was up to 1 X 10^{-5} M of nitrate concentration while LOD was averagely up to 5.7 X 10^{-7} M.

It can be concluded that this study had successfully produced a high sensitivity and reliable miniature nitrate sensor that can be applied in the field for PA activities. Extensive sensor performance study which includes operating temperature and pH range are recommended for wide application in PA and for better PA management of nitrate in soil determination.

REFERENCES

Adamchuk, V. I., Hummel, J. W., Morgan, M. T. & Upadhyaya, S. K. (2004). On-the-go soil sensors for precision agriculture. *Computers and Electronics Agriculture, 44,* 71-91.

Amemiya, S. (2007). Potentiometric ion-selective electrodes: *Handbook of Electrochemistry, 7,* 261-294.

Bakker, E. (2005). Ion-selective electrodes: Liquid membrane. In *Encyclopedia of Analytical Science* (Vol. 9, pp. 509-515). Auburn, AL. Encyclopedia Analytical Science.

Blonquist Jr, J. M, Jones, S. B. & Robinson, D.A. (2006). Precise irrigation scheduling for turf grass using a subsurface electromagnetic soil moisture sensor. *Aquaculture Water Management, 84,* 153-165.

Bobacka, J. & Ivaska, A. (2007). Ion sensors with conducting polymers as ion-to-electron transducers. *Comprehensive Analytical Chemistry, 49,* 73-85.

Bogrekci, I. & Gadwin, R. J. (2007). Development of a mechanical transducer for real-time soil tilth sensing. *Biosystem Technology, 98,* 127-137.

Buck, R. P. & Lindner, E. (1994). Recommendations for nomenclature of ion-selective electrodes. *Pure & Applied Chemistry, 66,* 2527-2536.

Careem, M. A., Velmurugu, Y., Skaarup, S. & West, K. (2006) A voltammetry study on the diffusion of counter ions in polypyrrole films. *Journal of Power Source, 159*, 210-214.

Cranny, A., Harris, N. R., White, N. M, Barret-Lennard, E., Coles, N., Rivers, M., Smettem, K. & Wu, J. (2012). Screen-printed sensors for chloride measurement in soils. *Procedia Engineering, 47*, 1157-1160.

De Marco, R. & Clarke, G. (2009). Ion-selective electrodes. In *Encyclopedia of Electrochemical Power Sources* (Vol.7, pp. 103-109) Perth, WA: Encyclopedia Electrochemical Power Sources.

Dechorgnat, J. I., Nguyen, C. T., Armengaud, P, Jossier, M., Diatloff, E., Filleur, S. & Daniel-Vedele, F. (2011). From the soil to the seeds: the long journey of nitrate in plants. *Journal of Experimental Botany, 62*, 1349-1359.

Dimeski, G., Badrick, T. & St John, A. (2010). Ion-selective electrodes (ISEs) and interferences - A review. *Clinica Chimica Acta, 411*, 309-317.

Escorihuela, M. J, Chanzy, A., Wigneron, J. P. & Kerr, Y. H. (2010). Effective soil moisture sampling depth of L-band radiometry: A case study. *Remote Sensing Environment, 114*, 995-1001.

Florinel-Gabriel, B. (2012). *Chemical sensors and biosensors: Fundamental and applications*. United Kingdom, UK: John Wiley & Sons, Ltd.

Frag, E. Y. Z., Ali, T.A., Mohamed, G.G. & Awal, Y. H. H (2012). Construction of different types of ion-selective electrodes. Characteristic performance and validation for direct potentiometric determination of orphenadrine citrate. *International Journal of Electrochemical Science, 7,* 4443-4464.

Gertsis, A., Fountas, D., Aepasanu, I. & Michaloudis, M. (2013). Precision agriculture applications in a high density olive grove adapted for mechanical harvesting in Greece. *Procedia Technology, 8*, 152-156.

Guilbault, G. G. (1986). Recommendations for publishing manuscripts on ion-selective electrodes. *Pure & Applied Chemistry, 53*, 1907-1912.

Kweon, G. & Maxton, C. (2013). Soil organic matter sensing with an on-the-go optical sensor. *Biosystem Engineering, 115*, 66-81.

Makarychev-Mikhailov, S. Shvarev, A. & Bakker, E. (2008). New trends in ion-selective electrode. *Electrochemical, Sensors, Biosensors and Their Biomedical Applications, 4*, 71-113.

Maleki, M. R., Mouzen, A. M., Ramon, J. & De Baerdemaeker, J (2007). Optimisation of soil VIS-NIR sensor-based variable rate application system of soil phosphorus. *Soil & Tillage Research, 94,* 239-250.

Mei-Rong, H., Gou-Li, G., Yong-Bo, D., Xiao-Tian, F. & Rong-Gui, L. (2012). Advanced solid-contact ion-selective electrode based on electrically conducting polymers. *Chinese Journal of Analytical Chemistry, 40,* 1454-1460.

Meyerhoff, M. E. & Opdycke, W. N. (1986). Ion-selective electrodes. *Advances in Clinical Chemistry, 25*, 1-47.

Mulla, D. J. (2013). Twenty five years of remote sensing in precision agriculture: Key advances and remaining knowledge gaps. *Biosystem Engineering, 114*, 358-371.

Murata, H., Futugawa, M., Kumazaki, T. Siagusa, M. Ishida, M. & Sawada, K. (2014). Millimeter scale sensor array system for measuring the electrical conductivity distribution in soil. *Computers and Electronics Agriculture, 102*, 43-50.

Oliver, M. A., Bishop, Thomas F. A. & Marchant, B. P. (Eds.) (2013). *Precision Agriculture for Sustainability and Environmental Protection*, New York, NY: Routledge.

Osakai, T., Sato, Y., Imoto, M & Sakaki, T. (2012). Interpretation of the potential response of PVC membrane ion-selective electrodes based on the mixed potential theory. *Journal of Electroanalytical Chemistry, 668*, 107-112.

Paczosa-Bator, B. (2012). All-solid-state selective electrodes using carbon black. *Talanta, 93*, 424-427.

Patois, T., Lakard, B., Monney, S., Roizard, X. & Fievet, P. (2011). Characterization of the surface properties of polypyrrole fils: Influence of electrodeposition parameters. *Synthetic Metals, 161*, 2498-2505.

Ping, J., Wang, Y., Wu, J. & Ying, Y. (2011) Development of an all-solid-state potassium ion-selective electrode using graphene as the solid-contact transducer. *Electrochemistry Communications, 13,* 1529-1532.

Porras-Gutierrez, A. G., Frontana-Uribe, B. A., Gutierrez-Granados, S., Griveau, S. & Bedioui, F. (2013). In situ characterization by cyclic voltammetry and conductance of composites based on polypyrrole, multi-walled carbon nanotubes and cobalt phthalocyanine. *Electrochimica Acta, 89,* 840-847.

Quan, D. P., Quang, C. X., Duan, L. T. & Viet, P. H. (2001). A conductive polypyrrole based ammonium ion-selective electrode. *Environmental Monitoring and Assessment, 70,* 153-165.

Ramanavicius, A., Ramananviciene, A. & Malinaukas. A. (2006). Electrochemical sensors based on conducting polymer polypyrrole. *Electrochemical Acta, 52,* 6025-6037.

R.W. Cattrall, J.W & Freiser, H. (1971) Coated wire ion-selective electrodes. *Analytical Chemistry, 43,* 1905-1906.

Telting-Diaz, M & Qin, Y. (2006). Potentiometry. *Comprehensive Analytical Chemistry, 47,* 625-659.

Vetelino J. & Reghu, A. (2011). *Introduction to sensors*. Florida, FL. CRC Press.

Vonau, W., Oelßner, W., Guth, U. & Henze, J. (2010). An all-solid-state reference electrode. *Sensors and Actuators B, 144*, 368-373.

Woo, S., Dokko, K. & Kanamura, K. (2008). Composite electrode composed of bimodal porous carbon and polypyrrole for electrochemical capacitors. *Journal of Power Source, 185*, 1589-1593.

Yin, T. & Qin, W. (2013). Applications of nanomaterials in potentiometric sensors. *Trends in Analytical Chemistry, 5*, 79-86.

Zhou, M., Zhu, B., Butterbach-Bahl, K., Wang, T., Bergmann, J., Bruggemann, N., Wang, Z., Li, T. & Kuang, F. (2012). Nitrate leaching, direct and indirect nitrous oxide fluxes from sloping cropland in the purple soil area, southwestern China. *Environmental Pollution, 162*, 361-368.

Zook, M. J., Langmaier, J. & Lindner, E. (2009). Current-polarized ion-selective membrane: The influence of plasticizer and lipophilic background electrolyte on concentration profiles, resistance and voltage transients. *Sensors and Actuators B: Chemical, 136*, 410-418.

Zubrowska, M., Wroblewski, W. & Wojciechowski, K. (2011). The effect of liphophilic salts on surface charge in polymeric ion-selective electrodes. *Electrochimica Acta, 56*, 6114-6122.